THE ASTROPHYSICAL JOURNAL, 330:91–104, 1988 July 1

SOFT X-RAY VARIABILITY AND THE COVERING FRACTION OF ACTIVE GALACTIC NUCLEI

KENNETH W. WACHTER,[1] MICHAEL A. STRAUSS,[2,3] AND ALEXEI V. FILIPPENKO[3]
University of California, Berkeley
Received 1987 October 12; accepted 1987 December 15

ABSTRACT

The intensity of soft X-rays (0.2–2 keV) emitted by some active galaxies is observed to vary on short time scales, from tens of minutes to days. In low-luminosity sources, these variations may be due in part to the motions of dense clouds in the broad-line region. The clouds partially block our line of sight to the X-ray emitting source, thought to be the inner regions of an accretion disk around a central black hole.

We derive the autocovariance function of the uncovered area for a model of a circular source region and circular, Poisson-distributed, moving clouds with random directions and a given speed. We assume that the clouds are optically thick in the energy band used, so that the flux received is directly proportional to the uncovered area. Comparison of this model with soft X-ray light curves and measurements of the broad-line cloud covering fraction yields estimates of the sizes of the clouds and the source. Measurements of the flux of the broad component of Hβ, or of the total X-ray flux, can both be used to estimate the value of the electron density in the broad-line clouds. We show that our results are rather insensitive to the assumed radial dependence of the surface brightness of the source, but are quite sensitive to a large dispersion in cloud sizes. The effect of finite optical depth of the clouds is also important. Although the current literature on soft X-ray light curves of active galactic nuclei is sparse, this formalism will be ideal for the analysis of data obtained with *EXOSAT* and *AXAF*.

Subject headings: galaxies: nuclei — galaxies: Seyfert — galaxies: X-rays — X-rays: sources

I. INTRODUCTION

A large fraction of bright QSOs, BL Lac objects, and Seyfert nuclei (hereafter collectively called active galactic nuclei, or AGNs) have been detected at X-ray energies (e.g., Elvis *et al.* 1978; Tananbaum *et al.* 1978; Canizares *et al.* 1986). Indeed, X-ray emission may be one of the more universal properties of AGNs (Elvis and Lawrence 1985).

The observed X-ray fluxes of many AGNs vary, with typical time scales that range from minutes to days and longer, depending on the object's type (Barr and Mushotzky 1986; Canizares *et al.* 1986; Warwick 1986; Pounds and Turner 1987). Intrinsically luminous QSOs usually have long periods. Narrow emission-line galaxies, on the other hand, vary on time scales of days (Mushotzky 1982), and a few low-luminosity Seyfert 1 nuclei such as NGC 6814 and NGC 4051 vary over periods of $\sim$0.1–1 hr (Pounds 1979; Tennant *et al.* 1981; Tennant and Mushotzky 1983; Lawrence *et al.* 1985). Significant changes have been seen over time scales as short as 1 minute in certain luminous BL Lac objects (e.g., H0323+022, Feigelson *et al.* 1986; OJ 287, Worrall *et al.* 1982), but they are probably related to beaming of the radiation (Blandford and Königl 1979; Phinney 1985) rather than to *intrinsic* variations of the X-ray luminosity. Beaming is unlikely to be important in type 1 Seyfert galaxies, whose X-ray fluxes are thought to vary due to changes in the rate at which a central black hole accretes matter from a surrounding disk (see, for example, Lightman, Giacconi, and Tananbaum 1978).

The variability of *soft* X-rays (0.2–2 keV) in some low-luminosity type 1 Seyfert galaxies may partly be due to another mechanism: dense clouds of gas in the broad-line region (BLR) moving across our line of sight to the X-ray emitting portions of the accretion disk (Reichert, Mushotzky, and Holt 1986, hereafter referred to as RMH; Lawrence and Elvis 1982; Halpern 1984). As the clouds move, the covering fraction changes stochastically. Evidence for partial covering of the X-ray source has been deduced from soft X-ray spectra by Holt *et al.* (1980) and Reichert *et al.* (1985).

This variability is not associated with changes in the intrinsic luminosity of the AGN, yet it may dominate the observed variability in some objects. If so, the soft X-ray light curve can be used, together with suitable models, to constrain some of the physical and geometric properties of the clouds and of the central source of X-ray energy. In this paper we consider the mathematical aspects of this problem and present formulae to help in the interpretation of future observations of soft X-ray variability. RMH have already discussed the two limiting cases of many small clouds on a larger source, and of one large cloud on a smaller source. Here we deal with situations between these two extremes.

In the next section we describe the basic principles behind this idea. Sections III and IV derive the autocovariance function of the uncovered area for circular clouds, moving with fixed speed, in uniformly distributed directions, from Poisson-distributed centers over a circular source in the plane. The derivation is the counterpart, for dynamic caps, of the variance formulae for fixed caps in the plane that go back to Moran and Fazekas de St. Groth (1962) and which underlie the elegant theory of random mosaics developed by Hall (1985). In § V, the closed-form formulae are evaluated over a range of covering fractions, cloud sizes, and X-ray source sizes,

[1] Department of Statistics.
[2] Department of Physics.
[3] Department of Astronomy.

providing the basis from which to estimate these quantities from observations of the soft X-ray variability of specific objects. Electron densities can also be calculated from observations of the flux of the broad component of Hβ, or of the total X-ray flux. Section VI analyzes the sensitivity of such estimates to violations of the geometric assumptions. We summarize our results in § VII.

II. MOVING CLOUDS AND SOFT X-RAY VARIABILITY

A distinguishing feature of the optical and ultraviolet spectra of QSOs and Seyfert 1 nuclei is the presence of broad, permitted emission lines; see Osterbrock and Mathews (1986) for a recent review. The widths are almost certainly produced by bulk motions of line-emitting gas, typical speeds being ~ 3000 km s^{-1}. Comparison of the observed luminosities of the emission lines with the results of photoionization models shows that the gas occupies only a small fraction of the total volume of the BLR in which it is located (e.g., Davidson and Netzer 1979). Thus, the gas is probably distributed in small "clouds" around the central source of ionizing radiation. The fraction of the sky covered by these clouds, as viewed by the central object (thought to be a massive black hole), must be small ($\lesssim 5\%$–10%) in luminous QSOs, since few high-redshift QSOs exhibit a dramatic cutoff in their X-ray spectra below ~ 3 keV. Low-luminosity AGNs [$L_X(2\text{–}10\ \text{keV}) \lesssim 3 \times 10^{43}$ ergs s^{-1}], on the other hand, typically have much larger covering fractions. In some cases these approach unity, as is evidenced by the strong absorption of soft X-rays in their X-ray spectra (Lawrence and Elvis 1982; Mushotzky 1982; Reichert *et al.* 1985).

Based on the absence of prominent forbidden lines and the presence of semipermitted lines, the gas density within the clouds has generally been quoted as $n \approx 10^9$–10^{10} cm^{-3}. This argument may be vitiated by collisional effects in the optically thick regime, making the true value at least one order of magnitude higher (see, for example, Puetter 1986 and references therein). X-ray spectra of AGNs (Reichert *et al.* 1985; Halpern 1984) and photoionization models of the BLR (Kwan and Krolik 1981; Halpern 1982) indicate that the clouds always have column densities of $N_H \approx 10^{22}$–10^{23} cm^{-2}. Hence, if the clouds have density $n \approx 5 \times 10^9$ cm^{-3}, their radii are 10^{12}–10^{13} cm, independent of the luminosity of the AGN. A range of 10^{11}–10^{14} cm, however, is not excluded by observations.

How do these radii compare with the expected sizes of the X-ray emitting regions? The X-rays are believed to come from the hottest, innermost portion of the accretion disk, within distances of $\sim 5R_s$ (e.g., Shakura and Sunyaev 1973), where $R_S = 2GM/c^2$ is the Schwarzschild radius of the putative black hole. If all AGNs accrete matter at their Eddington limit, as may be the case in luminous QSOs (Malkan 1983), then $M \approx (8 \times 10^5) L_{44}\ M_\odot$, where the bolometric luminosity is $L_{44} \times 10^{44}$ ergs s^{-1}. Thus, the radius of the X-ray source is $d \approx 10^{12} L_{44}$ cm. If AGNs actually accrete at sub-Eddington rates (Wandel and Yahil 1985; Wandel and Mushotzky 1986), the central mass and the size of the disk must both be correspondingly larger. (Note, however, that Bassani, Dean, and Sembay [1983] rederive the Eddington limit, taking into account various relativistic effects and beaming, and find a higher value than that obtained in the usual manner.)

These calculations show that the X-ray emitting region of low-luminosity sources may be comparable to, or smaller than, a broad-line cloud, as in the limiting case of small source and large cloud treated by RMH. A cloud of radius 10^{12} cm, for example, moving across our line of sight with a speed of 3000 km s^{-1}, would traverse a source of comparable size ($L_{44} \approx 1$) in 1 hr, occulting a fraction of it that depends on the alignment between the source and the cloud. A less luminous AGN, with a smaller disk, would be occulted more rapidly, and thus would have a greater probability of being completely eclipsed by a single passing cloud, with a correspondingly higher amplitude of fractional flux variation. An example of such an event may be the 2000 s intensity dip observed in NGC 4151 by Whitehouse and Cruise (1985). Very luminous QSOs, on the other hand, have large disks (10^{14}–10^{15} cm), so an individual cloud cannot block a great fraction of the X-rays. Any variability is the result of the combined contributions of many small clouds, as in the small-cloud limit treated by RMH. Indeed, we find the amplitude of fractional variation to be smallest, and the time scales longest, in the most luminous QSOs (Lawrence and Elvis 1982; RMH), as expected if this mechanism is dominant. (Of course, the intensity of AGNs may also vary for other reasons; see § I.)

The nature of the cloud trajectories in the BLR is not known with certainty. Velocities are measured along our line of sight. We have equated them to velocities across our line of sight, which is appropriate if the clouds move in Keplerian orbits. A component of infall or outflow can be accommodated simply by reducing the value of our velocity parameter, v. Under the assumption of circular Keplerian orbits, the ratio of cloud orbital radius to source radius is ~ 1000 for velocities of 3000 km s^{-1}. The nearest approach of clouds to the source cannot be very much less, even if eccentricity, infall, or outflow are present. Such distances from source to BLR render the curvature of any orbit as projected across our line of sight entirely negligible and permit the motions to be treated as rectilinear in projection. This simplification is convenient, although not necessary, to the methods presented in § IV. In order to preserve the Poisson hypothesis, we also ignore the possibility that a given cloud might be sufficiently long lived to pass through our line of sight more than once. This is reasonable, since a number of processes can destroy clouds on a dynamical time scale (e.g., Krolik, McKee, and Tarter 1981; Osterbrock and Mathews 1986).

The optical depth, at frequency ν, of hydrogen with a column density of N_H cm^{-2} is given by (Longair 1981)

$$\tau_\nu = 2 \times 10^{-22} \left(\frac{h\nu}{1\ \text{keV}} \right)^{-8/3} N_H .$$

Thus, $\tau \approx 1$ at 2 keV for a column density of 3×10^{22} cm^{-2}. We will assume in our analysis that the clouds are completely opaque to soft X-rays. The relevant band for observations will therefore be defined at the low-energy end by absorption within our own Galaxy along the line of sight, and at the high-energy end by the measured column density of the broad-line clouds.

Of course, the broad-line clouds are largely transparent to hard X-rays because N_H is much less than the Compton column density of $\sim 10^{25}$ cm^{-2}. In this regard, X-ray spectra of NGC 4151 (Barr *et al.* 1977; Holt *et al.* 1980) and MR 2251−178 (Halpern 1984) have shown dramatic changes in the soft X-ray flux between measurements separated by a year, while the hard X-ray flux remained unchanged. (The latter object, however, is a rather luminous X-ray source; it goes against the general trend discussed earlier. Also, the case for NGC 4151 has become more uncertain with recent *EXOSAT* observations; see below.) This provides some

evidence against intrinsic variation of the X-ray source, and supports the idea of variability in covering fraction by broad-line clouds. Furthermore, M81 has exhibited soft X-ray variability on time scales of 600 s to several years (Barr and Giommi 1985; Barr *et al.* 1985), while the flux of the broad component of Hα remained steady (Filippenko and Sargent 1988), again suggesting that the ionizing radiation does not vary intrinsically. On the other hand, Lawrence *et al.* (1985) show that the X-ray light curves of NGC 4051 at 0.04–2 keV and at 2–6 keV have a very high correlation, implying that the rapid variability in this low-luminosity source is probably intrinsic. A similar correlation between hard and soft X-ray light curves is seen in MCG 6-30-15 (Pounds and Turner 1987). The relative contributions of extrinsic and intrinsic variability are certainly not the same in different objects.

The case of NGC 4151 deserves further discussion. Although Holt *et al.* (1980) fitted the X-ray spectrum with a power law, absorbed by broad-line clouds covering 90% of the source, more recent *EXOSAT* measurements have shown that this picture is incomplete. Pounds *et al.* (1986; see also Perola *et al.* 1986) model the spectrum with components having two different absorbing columns, and an additional soft X-ray excess seen in the low-energy telescope (0.15–2 keV). The soft component did not vary during a period when the 2–10 keV flux changed by a factor of 3, implying that it arises from a physically distinct region of the AGN. Soft X-ray excesses are found in a large variety of AGNs (e.g., Branduardi-Raymont 1986; Wilkes and Elvis 1987; Filippenko and Halpern 1988), and must be taken into account in a complete model of partial covering and soft X-ray variability. Here we will simply assume that the soft X-rays all arise from the central source.

The average radius of clouds, as noted above, is uncertain to a factor of at least 10, and perhaps as much as 1000. In most AGNs, the radius of the X-ray source is also uncertain, since no *direct* measurements of the central black hole's mass have yet been made. We shall show below that predictions of cloud radius and source radius can be obtained with our model from accurate measurements of the observed autocovariance of the soft X-ray light curve, if the flux variations are entirely due to the motion of clouds across our line of sight. These predictions require a measurement of the mean covering fraction from the soft X-ray absorption spectrum (e.g., Holt *et al.* 1980; Reichert *et al.* 1985), a method of quite limited precision, as we saw above. We also require some assumption about the extent of randomness in cloud sizes, as discussed in § VI. Finally, it is assumed that the broad-line clouds are completely opaque to soft X-rays; the effect of finite optical depth can be taken into account without much difficulty, however, and will be discussed in § VI.

The autocovariance function allows one to define an unambiguous index of the time scale of variability, but it requires a long, well-sampled, and uninterrupted light curve (Schwartz 1987). Although Lawrence *et al.* (1987) have shown that the power spectrum of the soft X-ray light curve of NGC 4051 is a power law, implying that one cannot define *any* characteristic time scale of variability, we saw in § II that the variability of this source is intrinsic. Objects in which an unambiguous time scale is absent (i.e., the variability is fractal), or in which there is correlated soft and hard X-ray variability, cannot easily be analyzed in the manner described here.

If, in addition to the soft X-ray light curve, one has a measurement of the flux in the broad component of Hβ, one can use the method of Wandel and Yahil (1985) in conjunction with our model to derive an electron density (n_e) in the broad-line clouds. Of course, one must be careful to keep in mind the uncertainties and assumptions associated with this technique (Filippenko 1988).

All soft X-ray light curves available in the literature are of insufficient quality for immediate realization of these goals. With the demise of *EXOSAT*, it is currently difficult to obtain large quantities of new observational results to compare with the formalism presented here. On the other hand, the Japanese *Ginga* and Soviet *Kvant* X-ray telescopes may be capable of obtaining the necessary data for bright AGNs. Moreover, suitable light curves were obtained with *EXOSAT* for a few objects, and are starting to be published (e.g., Lawrence *et al.* 1987; Warwick 1986; Pounds and Turner 1987). Finally, development and criticism of estimation methods is important for planning observational strategies, before new X-ray satellites such as *ROSAT* and *AXAF* are launched.

III. THE POISSON MODEL

The model we propose treats the centers of the clouds projected onto the plane perpendicular to our line of sight to the AGN, at a fixed point in time, as a statistical Poisson process. The content of the Poisson specification is twofold. First, the locations of the (projected) centers are independently and uniformly distributed in the plane. Second, the total number of centers in a given region is not fixed; rather, it is a random variable with a Poisson distribution. These assumptions together entail the desirable property that the number of centers in any given subregion is independent of the number in any disjoint subregion at a fixed time.

Under the reasonable hypothesis that the actual cloud centers are distributed independently and isotropically around the AGN, we require two conditions to realize the Poisson limit for the projected centers. The first is that the curvature of the orbits of the broad-line clouds be negligible in the region near our line of sight, thereby guaranteeing the uniform distribution of centers on the plane. That is, "limb brightening" due to the fact that we are looking at a spherical distribution in projection should be small over the region containing those clouds that might move across our line of sight in the relevant time interval. If the innermost part of the BLR lies 1000 source radii from the source (§ II), the resulting nonuniformity in the distribution of clouds 10 times larger than the sources does not exceed 1%.

The second condition pertains to the randomness of the number of clouds. The region containing clouds that might cover the source in the relevant time interval occupies less than 10^{-4} of the celestial sphere as viewed from the AGN. For plausible values of mean covering fractions, the random number of centers lying in such a small subregion has a distribution indistinguishable from a Poisson distribution, even if the total number of clouds in the BLR is assumed to be constant on time scales of days or weeks.

With these conditions, we can go through the standard derivation of the mean covering fraction, f. Suppose that clouds, whatever their shape, are randomly oriented and have cross sections whose expected area equals the area of a circle of radius r. Imagine placing N cloud centers independently and uniformly on the surface of the celestial sphere, of area $\mathscr{A}$, around the AGN. Pick a point P on the surface. There is a probability $p = \pi r^2/\mathscr{A}$ that the first cloud covers the point P, and a probability $1 - p$ that it does not. Since the clouds are placed independently, the probability that neither the first nor the second clouds cover P is $(1 - p)^2$. Given N, the probability that all N clouds miss P is therefore $(1 - p)^N$. If p is small and the number of clouds is constant and large, this probability can be approximated as $e^{-pN} + \mathcal{O}(e^{-Np^2/2})$. If the number of clouds is random and Poisson-distributed, this probability,

on average, is exactly equal to e^{-pN}, provided N is then interpreted as the mean number of clouds. In either case, the mean covering fraction, equal to the probability that an arbitrary point is not missed, may be taken to be

$$f = 1 - e^{-\pi r^2 N/\mathscr{A}} = 1 - e^{-\lambda \pi r^2} . \tag{1}$$

Here $\lambda \equiv N/\mathscr{A}$ is the mean number of clouds per unit area—that is, the intensity of the Poisson process that deposits cloud centers. The covering fraction depends only on the product of λ and the "forbidden" area πr^2, from which cloud centers must be absent to avoid covering a given point. We emphasize that the observed energy band is assumed to be one in which the clouds are completely opaque, so that the flux is directly proportional to the uncovered fraction. The consequences of dropping this assumption are discussed in § VI.

When the mean covering fraction is close to unity, the asymptotic theorems of Hall (1985) give approximations for the moments of the size and number of interstices between the clouds through which the X-ray source can be seen. When the covering fraction is large, the individual interstices are much smaller than the clouds, and the curvature of the segments that make up their sides becomes negligible. Thus, the distribution in area of the interstices is directly related to that of the polygons formed by placing random lines on a plane. To use such a relationship, we need to calculate how the intensity of the random line process depends on the radius of clouds and on the number of cloud centers per unit area.

We derive the relationship for the simple case of uniform circular clouds of radius r. Imagine a point P in an interstice. How many clouds have boundaries that come within a distance ρ of P? In order for P to be in an interstice, the must be no cloud centers within a distance r—otherwise, P would be covered. Those clouds whose boundaries come within ρ of P, but do not cover P, have centers between r and $r + \rho$ from P, in a ring of area $2\pi r\rho + \pi\rho^2$. Multiplying this area by λ, the expected number of cloud centers per unit area, gives the expected number of cloud boundaries that come within ρ of P. In the limit of small ρ/r, the expected number is $2\pi\lambda r\rho$. We equate this to the expected number of lines in the analogous process of random lines in the plane.

One can describe lines in a plane by the polar coordinates (p, θ) of the foot of the perpendicular from the origin onto the line. The intensity of the line process, κ, is defined as the number of lines in a unit square of the (p, θ) phase space (Kendall and Moran 1963, § 3). A Poisson line process is a set of random lines whose coordinates in this phase space are Poisson distributed. Since there are $2\pi\rho r\lambda$ lines in our process within a perpendicular distance ρ of a given point, and within all 2π radians of angle, we have $\kappa = r\lambda$.

A rigorous version of these arguments is found in Hall (1985). He proves this result for clouds of arbitrary shape and a distribution of sizes, if $2\pi r$ in the above argument is replaced by $2\pi\tilde{r}$, the expected value of the perimeter of a cloud.

In the Appendix, we show that the expected area of the polygons formed between the lines of a Poisson line process of intensity κ is

$$S = \frac{1}{\pi\kappa^2} . \tag{2}$$

This is reasonable, since κ has the dimensions of number (of lines) per unit distance (from a point), and the expected area of interstices decreases as either the number density or the size of clouds increases.

If β is defined to be the radius of a circle of area equal to the expected area of an interstice, it follows that

$$\pi\beta\tilde{r} = 1/\lambda = \mathscr{A}/N . \tag{3}$$

Using Equation (1) to solve for N in terms of the expected covering fraction, we obtain the ratio of typical interstice radius to the cloud perimeter parameter $\tilde{r}$ as

$$\frac{\beta}{\tilde{r}} = \frac{(r/\tilde{r})^2}{\ln\left[(1-f)^{-1}\right]} . \tag{4}$$

Given circular clouds all of the same radius, the numerator on the right-hand side is unity.

For sources with high covering fractions, we can use equation (4) to estimate a period over which variability might be observed. This is the time scale on which one of the interstices can be obliterated by the motion of an adjoining cloud. As an example, imagine an AGN with a measured covering fraction of 90%. Equation (4) predicts interstices of radius ~ 0.4 times the radius of the clouds. We take as a typical cloud speed $v \approx 3000$ km s^{-1}. If the broad-line clouds are 10^{11} cm across, an interstice could be covered in 2.4 minutes. The corresponding time if they are 10^{14} cm across, at the other extreme of the suggested range (§ II), is ~ 4 hr. These values are within the time scales over which variability has actually been observed in some AGNs.

Equations (1) and (3) also allow us to calculate the ratio of the expected number of interstices (N') to the expected number of clouds, a relation valid as long as N' is neither close to zero nor inordinately large:

$$\frac{N'}{N} = (1-f)\frac{\tilde{r}}{\beta} . \tag{5}$$

For 90% covering, there would be around one-fifth as many interstices as clouds; for 99% covering, around one-twentieth.

The covering fractions of AGNs are generally believed to range from ~ 0.05 in luminous QSOs to ~ 1 in low-luminosity Seyfert 1 nuclei. It is well to bear in mind, however, that the expected covering fraction cannot be too close to unity if clouds are larger than a source, or the source would be observed in soft X-rays only on rare occasions. For instance, if the clouds and the source have equal size, a covering fraction of 99% could occur with an average of only 4.6 cloud centers in front of a source. Equation (5) then predicts ~ 0.2 interstices on the source. This case oversteps the limits of validity of equation (5), but it is nonetheless clear that the source would be uncovered only a small fraction of the time.

IV. THE AUTOCOVARIANCE FUNCTION

Detailed predictions of variability characteristics from our geometric model require computation of the autocovariance function, which gives the covariance between the area of the source uncovered by any cloud at time zero and the area uncovered at time t, as a function of t. Since the variance of the uncovered area, the mean square deviation from the mean, is independent of time, the autocovariance function is just the autocorrelation function multiplied by the variance. We assume that the clouds are completely opaque; this assumption is relaxed in § VI.

a) Notation

We define the following parameters:

λ—The intensity parameter, or mean number of cloud centers per unit area, when the cloud centers are taken to be a realization of a homogeneous Poisson process in the plane perpendicular to our line of sight to the source.

d—The radius of the assumed circular cross section of the X-ray source, whose uncovered portion is the variable of interest.

R—A radius of the assumed circular cross section of a given cloud, taken to be a random variable independent of the position of the cloud, with distribution given by the probability density function $h(R)$.

$\mathbf{E}$—Expectation value.

$r = (\mathbf{E}R^2)^{1/2}$—The radius of a circle whose area equals the expected area of the cross section of a cloud.

v—The speed of the clouds. This is the same for all clouds, which are assumed to move in straight, randomly oriented paths across the plane.

A and B—Points on the source, randomly chosen according to a radially symmetric density which reflects the X-ray surface brightness. The central source is assumed to be uniform in § V. We allow it to take other forms in § VI by varying the shape of the probability density function $g(w)$, for the ratio w of distance between A and B to source radius d.

$I(A, t)$—The indicator function of the event that the point A on the source is uncovered at time t; that is, let I take the value 1 when A is uncovered, and 0 otherwise.

b) Derivation

The distribution of cloud centers in the plane, placed according to a Poisson process at time zero with a constant intensity parameter λ, continues to be a Poisson process with the same constant λ at any later time, as long as the direction of motion of each cloud is randomly chosen from a uniform distribution of directions independent of position. This fact follows from Liouville's Theorem on the constancy of phase-space density under measure-preserving transformations in phase space (Goldstein 1980). Our phase space for a cloud's initial conditions has two real-valued coordinates for position in the plane, and one coordinate on the half-closed interval [0, 1) giving the angle of the velocity vector relative to some fixed axis as a fraction of 2π radians. Were it necessary to take into account the curvature of Keplerian orbits in the BLR, the derivation could be carried out in a phase space of generalized Hamiltonian coordinates.

For the case of a source with uniform surface brightness, the uncovered area at time zero is the surface integral $\int I(A, 0)dS_A$, and the uncovered area at time t is $\int I(B, t)dS_B$. Thus, the covariance between the areas uncovered at time zero and time t is

$$\mathrm{cov} = \mathbf{E}\iint I(A, 0)I(B, t)dS_A\, dS_B - \left[\mathbf{E}\int I(A, 0)dS_A\right]\left[\mathbf{E}\int I(B, t)dS_B\right]. \tag{6}$$

The expected uncovered area is the total area, πd^2, multiplied by the mean covering fraction in equation (1):

$$\mathbf{E}\int I(A, 0)dS_A = \int \mathbf{E}I(A, 0)dS_A = \int \mathbf{E}I(B, t)dS_B = \pi d^2 e^{-\lambda\pi r^2}. \tag{7}$$

The square of this quantity is the second term in the covariance. The first term requires finding an expression for $\mathbf{E}I(A, 0)I(B, t)$, the probability that every cloud fails to cover A at time zero and fails to cover B at time t. As in the derivation of f in § III, independence of cloud locations implies that

$$\mathbf{E}I(A, 0)I(B, t) = e^{-\lambda V}, \tag{8}$$

where V is the expected volume of the "forbidden" region of phase space—that is, the region of phase space which must be empty at time zero if a particular cloud, chosen at random, fails to cover A at time zero and fails to cover B at time t.

Suppose a cloud with randomly selected radius R has its center at a point C at time zero and moves to a point D, distance vt from C, at time t, as shown in Figure 1. Then the cloud's coordinates fall in the forbidden volume of phase space either if C falls inside a circle of radius R around A at time zero, or if D falls inside a circle of radius R around B at time t. The total forbidden volume is the sum of πR^2 times 1 (since the condition on C does not restrict the angle coordinate), plus another πR^2 for the region around D, minus the volume of the intersection of these two regions. It is the intersection which requires special attention.

The distance from A to B is wd by definition, and let z be the distance from B to C. We define the angles θ between the segments AB and BC, and ψ between the segments BC and CD; see Figure 1. For a given z, a cloud can belong to the intersection only if the angle θ satisfies an inequality based on the law of cosines:

$$(z - wd\cos\theta)^2 + (wd\sin\theta)^2 < R^2. \tag{9}$$

The measure $Q(z, wd, R)$ of this set of angles as a fraction of 2π radians, multiplied by $2\pi z$, is the length of the arc containing possible choices of C. A cloud with its position coordinates on this arc contributes to the intersection if the angle ψ, which gives its direction of motion, satisfies a similar inequality:

$$(z - vt\cos\psi)^2 + (vt\sin\psi)^2 < R^2. \tag{10}$$

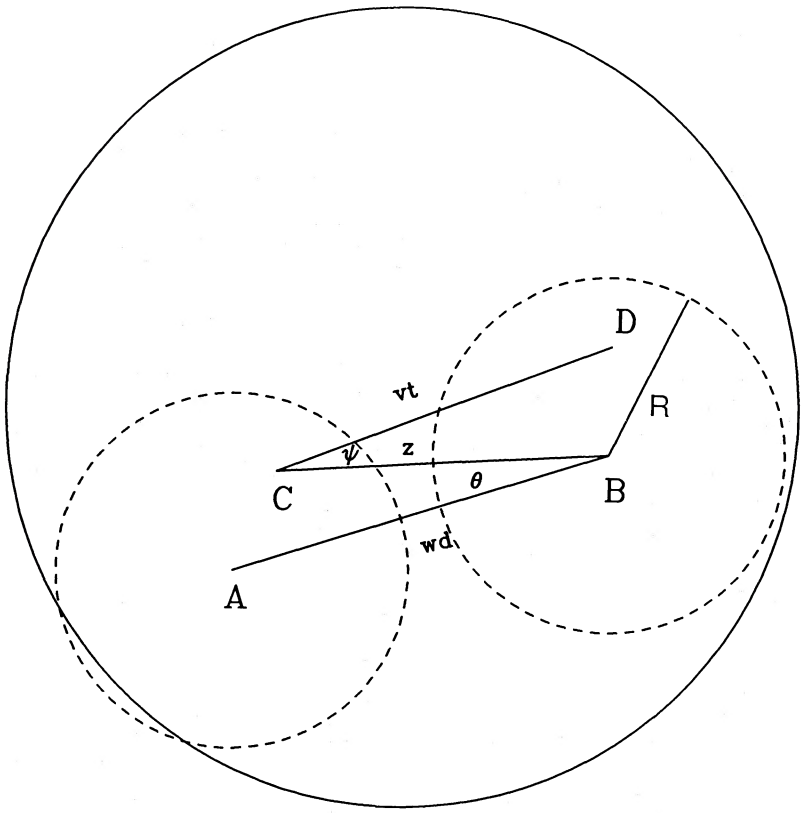

FIG. 1.—The geometry of the discussion in § IV. The large circle represents the X-ray source. Points A and B are randomly selected on it. A circular cloud with center C at time zero moves with velocity v to point D in time t. If this cloud has radius R, it covers both A at time zero and B at time t if, as shown here, C and D fall within circles of radius R around A and B, respectively.

The direction of motion of a cloud is independent of its position, so the total volume of the intersection is obtained by summing contributions for all values z of the distance from B to C:

$$\int Q(z, wd, r)Q(z, vt, r)2\pi z\, dz\ . \tag{11}$$

The function Q, which gives the measure of the angles satisfying the law of cosines, has the formal definition

$$\begin{aligned} Q(z, y, x) &= 0 \qquad \text{if} \quad (z - y)^2 > x^2\ , \\ Q(z, y, x) &= 1 \qquad \text{if} \quad (z + y)^2 < x^2\ , \\ Q(z, y, x) &= \left(\frac{1}{\pi}\right)\cos^{-1}\left(\frac{z^2 + y^2 - x^2}{2yz}\right) \qquad \text{otherwise}\ . \end{aligned} \tag{12}$$

The expected total volume of phase space, V, that must be empty of points of the Poisson process for A to be uncovered at time zero and B to be uncovered at time t, averaged over all values of the random cloud radius R, is given by

$$V = \int\left[2\pi R^2 - \int Q(z, wd, R)Q(z, vt, R)2\pi z\, dz\right]h(R)dR\ . \tag{13}$$

This expression depends on A and B only through the distance wd between them, and we may re-express the double surface integral in equation (7) in terms of the density $g(w)$ of w, which in the case of a source of uniform surface brightness takes the form

$$g(w) = \frac{d}{dw}\iint Q(a, b, w)4ab\, da\, db\ . \tag{14}$$

For other source profiles there are corresponding expressions. In terms of $g(w)$ we find

$$\mathbf{E}\iint I(A, 0)I(B, t)dS_A\, dS_B = \int \mathbf{E}I(A, 0)I(B, t)g(w)dw\ , \tag{15}$$

and the final answer for the autocovariance function is then

$$\mathrm{cov} = (\pi d^2)^2 e^{-2\lambda\pi r^2}\left[\left[\int g(w)\left\{\exp\left[\lambda\iint h(R)Q(z, wd, R)Q(z, vt, R)2\pi z\, dz\, dR\right]\right\}dw - 1\right]\right]. \quad (16)$$

Since $\pi d^2 e^{-\lambda\pi r^2}$ is the mean uncovered area, the factor in double brackets is the ratio of the covariance to the squared mean of uncovered area, a quantity derivable from a well-sampled soft X-ray light curve. This factor multiplied by $(1-f)^2 = e^{-2\lambda\pi r^2}$, the covariance of fractional area uncovered, will be used extensively in the next section to derive values of d/r.

V. RELATING OBSERVATIONS TO THEORY

The formulae in § IV provide a basis for studying the effects of the mean covering fraction, and the relative sizes of source and clouds, on the variability of the soft X-ray intensity. We have evaluated the functions by numerical integration with 100-point grids using the *S* statistical system of Becker and Chambers (1984). In this section we assume the source to be of uniform brightness throughout its cross section, and we take the clouds to be of fixed radius r. The effect of varying these assumptions is discussed in § VI. The density, $g(w)$, was calculated by differencing the double integral in equation (14) on a 200 point grid, for w on the interval [0, 2].

A typical autocovariance function predicted from the model is shown in Figure 2 for the case of a source with twice the radius of a cloud. The mean covering fraction f is set at 50%, corresponding to a Poisson process intensity of 0.221 clouds per r^2 units of area by equation (1). The autocovariance of the fraction of the area of the source uncovered is shown as a function of the time lag in units of r/v. Thus, one time unit is the interval required for a cloud center to move one cloud radius. In Figure 2, the ordinate intercept of 0.037 (the autocovariance at zero time lag) is the variance of the fractional area uncovered. The standard deviation of the fractional area uncovered is thus 20% around a mean of 50%. Normalization by the ordinate intercept gives us the autocorrelation function, which remains near 1.0 only for small time lags and descends to a value of one-half at $t = \tau_{1/2} = 1.6r/v$.

This "half-life" of the autocorrelation function, $\tau_{1/2}$, will be our index of the time scale of variability throughout the investigation. For any Gaussian random process, the expected decay of a peak, m, above the mean at some time t is given by the autocorrelation multiplied by m. Though the process is not strictly Gaussian, the interpretation is a reasonable one, and the correlational half-life can be pictured as the half-life of the expected deviation from the mean after a given peak.

A predicted power spectrum can readily be computed from the autocovariance function. The predicted spectrum typically decreases monotonically from a finite value at the origin, like the one corresponding to Figure 2. Since soft X-ray light curves long enough to estimate power spectra at low frequencies are likely to be rare, we concentrate here on the autocovariance function.

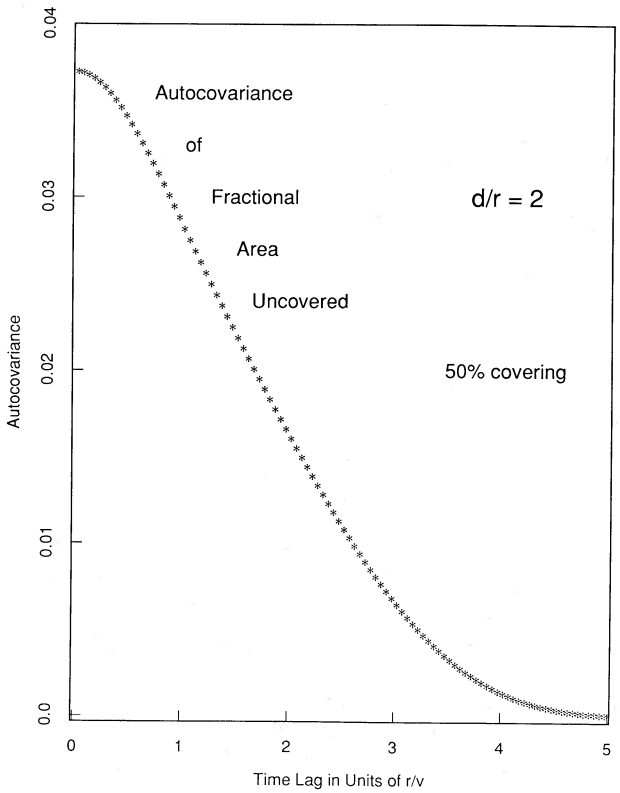

FIG. 2.—A typical example of an autocovariance function predicted by the model. The autocovariance of the fractional area of the source uncovered is shown as a function of the time lag in units of cloud radius divided by cloud velocity. This example takes the source radius to be twice the cloud radius and the mean covering fraction to be 50%.

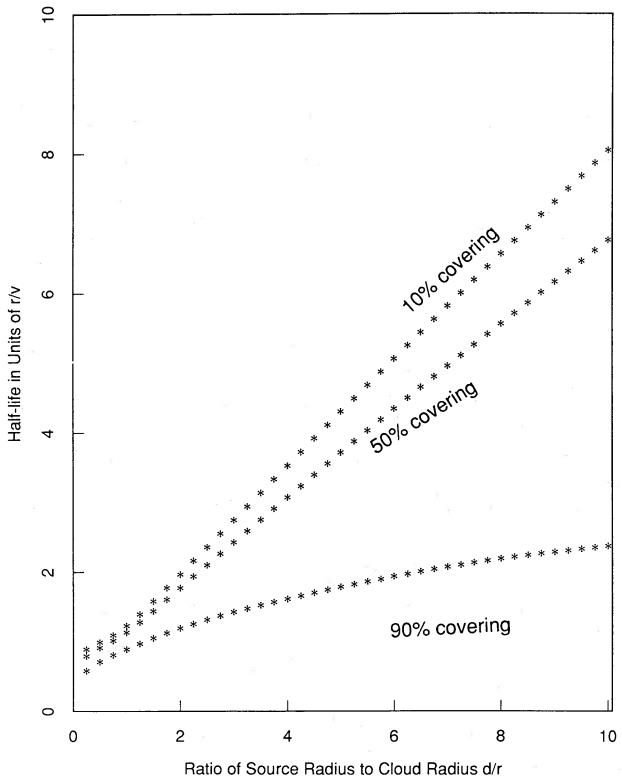

FIG. 3.—Predicted half-lives of autocorrelations in units of cloud radius divided by velocity, as a function of the relative size of the source and the clouds, for different covering fractions.

The dependence of the time scale of variability, as measured by the half-life of correlations, on the ratio of the source to cloud radii d/r, is shown in Figure 3. The three curves correspond to three values of the mean covering fraction f: 10%, 50%, and 90% covering. The middle curve, for 50% covering, is nearly linear, with a fit

$$\tau_{1/2} = 0.564r/v + 0.624d/v \ .$$

Hence, it takes a little over three correlational half-lives for a cloud center to traverse the diameter of the source when $f = 50\%$. Approximately 2.6 half-lives are necessary when covering is sparser ($f = 10\%$). When covering is denser ($f = 90\%$), the relationship is less linear and the coefficient on r/v is as important as that on d/v, thereby complicating the interpretation. The curves for $f = 50\%$ and 10% converge at the left toward ordinate intercepts around $\pi/4$. This is half the average duration of an eclipse, in units of r/v, when a single huge cloud passes across a tiny source. With higher mean covering fractions, the variability reflects multiple eclipses, and the intercepts and slopes of half-life versus d/r could scarcely be foreseen without the full geometric model.

The dependence of the variability amplitude on d/r is easiest to analyze if the quantity Ω, the ratio of mean uncovered area to the standard deviation of uncovered area, is used. On this reciprocal scale, Ω is an almost linear function of d/r when $d > r$ and f is moderate. When $f = 50\%$, we find $\Omega \approx 0.51 + 1.07d/r$. The ratio Ω is directly observable from the mean and standard deviation of an X-ray light curve, provided the light curve pertains only to *soft* X-rays, to which the clouds are fully opaque. It is convenient to divide Ω by the factor $1 - f$, yielding the reciprocal standard deviation of fractional area *uncovered*, as an alternate index of the variability amplitude.

Figure 4 is a contour plot of d/r and f as functions of the half-life, in units of r/v on the abscissa and of $\Omega/(1 - f)$ on the ordinate. This contour plot can be used with empirical data to estimate the radii d and r of source and clouds, respectively.

Although a fair number of well-sampled hard X-ray light curves exist in the literature (e.g., NGC 4151; Mushotzky, Holt, and Serlemitsos 1978), we are aware of well-sampled soft X-ray light curves only for MCG 6-30-15 (Pounds and Turner 1987) and NGC 4051 (Lawrence *et al.* 1987), both of which are inappropriate for this analysis (§ II). Pending publication of new *EXOSAT* data, we illustrate the application of Figure 4 with a hypothetical example. Consider a source with mean covering fraction $f = 90\%$. Assume a mean flux of 0.1 and a standard deviation of 0.04 in comparable units, for a ratio of 2.5. Suppose further that the autocorrelation function calculated from the soft X-ray light curve shows a half-life $\tau_{1/2}$ of 0.5 day (12 hr). Then the value of $\Omega/(1 - f)$, corresponding to the ordinate of Figure 4, is 25. The leftmost dotted vertical contour corresponds to $f = 90\%$, on which the ordinate of 25 corresponds to a value of $d/r = 5.3$. The expected half-life (abscissa) is therefore 1.7 in units of r/v. Equating $1.7r/v$ to the observed half-life of 0.5 day, and taking the velocity of the clouds v to be 3000 km s^{-1}, we find $r = 0.7 \times 10^{13}$ cm. Multiplying by $d/r = 5.3$ gives $d \approx 4 \times 10^{13}$ cm. Thus, the use of Figure 4 can lead directly to source and cloud size estimates that can be compared with the results of other, independent methods.

Given our predictions for d and r, we can solve for n_e in a variety of ways, and look for consistency between them. M81, discussed by Filippenko and Sargent (1988), provides a good example. This is the lowest luminosity Seyfert 1 galaxy known at optical

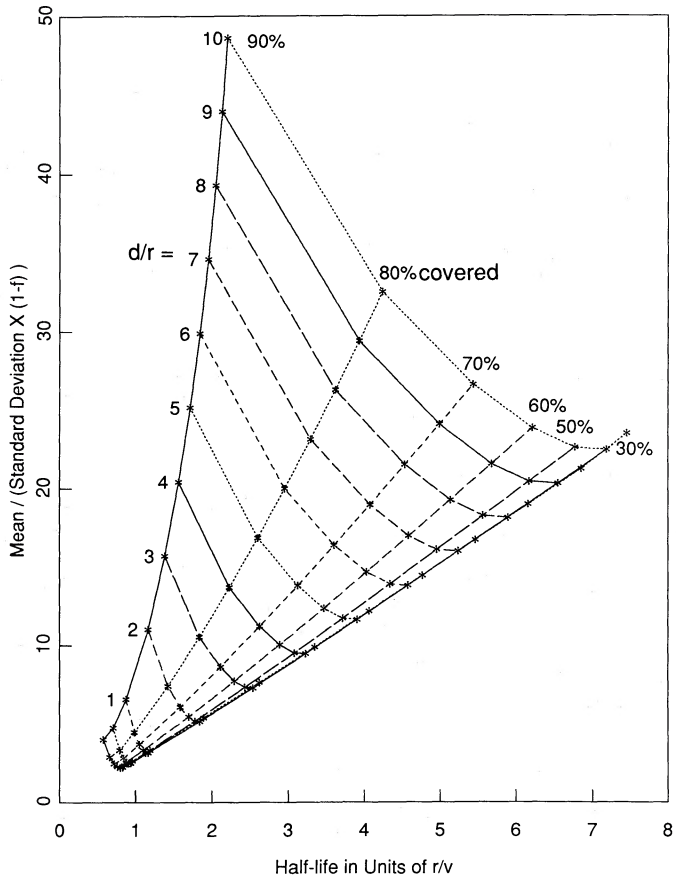

FIG. 4.—Contours of constant relative source size d/r, and of constant mean covering fraction f, on a plot of amplitude of variability vs. half-life. The index of amplitude of variability is the quantity $\Omega/(1-f)$, defined in the text. These contours assume that all clouds have the same radius. The contour plot can be used with empirical measurements of soft X-ray light curves to estimate sizes of source and clouds.

wavelengths, and one of the lowest at soft X-ray energies. Although a well-sampled soft X-ray light curve of this object does not exist in the literature, the relationship of d and r to n_e can be analyzed from existing data.

If $\mathscr{R}$ is an average distance from the central source to the broad-line clouds, then the definition of U, the ionization parameter, yields

$$\mathscr{R}^2 = \frac{L_X}{4\pi n_e c U}, \tag{17}$$

where L_X is the UV and X-ray photon flux ($E \geq 13.6$ eV) from the central source.[4] Using the relation of Shakura and Sunyaev (1973) between source radius d and its mass, and the virial theorem to relate the mass to the velocity and distance of the clouds, we find

$$d = 10\left(\frac{v}{c}\right)^2\left(\frac{L_X}{4\pi n_e c U}\right)^{1/2} = 1.8 \times 10^{11} v_3^2\left(\frac{L_{X48}}{n_{e9} U_3}\right)^{1/2} \text{ cm}, \tag{18}$$

where $v_3 = v/(1000 \text{ km s}^{-1})$, $L_{X48} = L_X/(10^{48} \text{ photons s}^{-1})$, $n_{e9} = n_e/(10^9 \text{ cm}^{-3})$, and $U_3 = U/10^{-3}$ (Halpern and Steiner 1983). For M81, Filippenko and Sargent (1988) quote $v_3 = 1.5$ and assume $U_3 = 1$, while Barr and Mushotzky (1986) give $L_{X48} = 3.7$, where we have assumed an average photon energy of 5 keV. Thus, we find $d = 7.8 \times 10^{11} n_{e9}^{-1/2}$ cm in M81.

Alternatively, we can calculate d from the relation between $\mathscr{R}$ and the broad Hβ luminosity L_β (Wandel and Yahil 1985), which gives

$$d = 1.4 \times 10^{13}\left(\frac{v}{c}\right)^2\left(\frac{L_\beta}{f N_\beta n_e}\right)^{1/2} = 1.56 \times 10^{13} v_3^2\left(\frac{L_{\beta 42}}{f n_{e9} N_{\beta 23}}\right)^{1/2} \text{ cm}, \tag{19}$$

where $L_{\beta 42} = L_\beta/(10^{42} \text{ ergs s}^{-1})$, f is the covering fraction, and $N_{\beta 23}$ is the column density of Hβ-emitting gas in units of 10^{23} cm^{-2}.

[4] Note that U may not be constant in the BLR if clouds having a given density exist at different distances from the central source, or if a range of densities is present at a given distance. Also, U is not a well-defined quantity in AGNs with large covering fractions because many clouds see only diffuse or scattered ionizing radiation. Detailed treatment of these complications is beyond the scope of this paper, especially in light of the current observational uncertainties in the relevant parameters.

The parameters of M81 assumed or derived by Filippenko and Sargent (1988) are $f = 1$, $N_{\beta 23} = 0.3$, and $L_{\beta 42} = 2.1 \times 10^{-4}$. Thus, $d = 9.3 \times 10^{11} n_{e9}^{-1/2}$ cm, in good agreement with the value quoted above. Furthermore, if we assume that the broad-line clouds are roughly circular, r is given by one half the ratio of N_β to n_e, or $r = 1.5 \times 10^{13} n_{e9}^{-1}$ cm.

Imagine that we have access to a well-sampled, soft X-ray light curve from which we can derive Ω and $\tau_{1/2}$. We showed above how we can use them to find d and r as functions of f, the covering fraction. But we have just found these two quantities in terms of n_e! Thus, we have two equations in two unknowns, and can solve for both n_e and f. In the happy situation where f is derived independently from measurements of the soft X-ray absorption, we can ask for consistency among all results. Lack of consistency either indicates that the fluctuations are not largely due to the movement of broad-line clouds, or perhaps that our model is too simplistic.

VI. SENSITIVITY TO ASSUMPTIONS

The estimates in § V depend on the assumptions that the source is of uniform surface brightness over its entire circular cross section, that the cloud radius is not random but fixed, and that clouds are totally opaque to X-rays in the monitored energy bands. Here we investigate the consequences of relaxing these constraints. We will continue, however, to assume that the clouds are circular; modifications introduced by elongated clouds are beyond the scope of this paper.

a) Source Surface Brightness

We may alter the assumption of the uniform surface brightness of the source simply by altering the density function, $g(w)$, for the distance between a pair of randomly selected points on the source. As an example, we consider the effect of substituting a source whose surface brightness declines linearly as a function of distance from the center, reaching zero at a distance d. Equation (14) is therefore modified to employ this "triangular" (tapered) profile function on a and on b, instead of the constant density $da\,db$.

Figure 5 illustrates the consequences of this change. The stars on the plot pertain to the uniform source, and the triangles to the tapered source. The half-life is plotted on the abscissa, and $\Omega/(1-f)$ on the ordinate, for various values of d/r and f. In comparison with the stars, the loci of triangles are compressed toward zero on both dimensions, since the "effective radius" of a source having a triangular profile is obviously somewhat smaller than the maximum radius d. The relationships between half-life and the ratio of mean to variance are in all cases so close to each other, however, that the assumption about source profile seems to be of little consequence for predictions.

b) Cloud Radii

If, on the other hand, the clouds obscuring the source have radii randomly distributed over a large range, predictions based on the assumption of a fixed common value of radius can be profoundly affected. Figure 6 shows predicted autocovariance functions as in Figure 2, but with different assumptions concerning the distribution of cloud radii. For each curve, the quantity ln R is given a

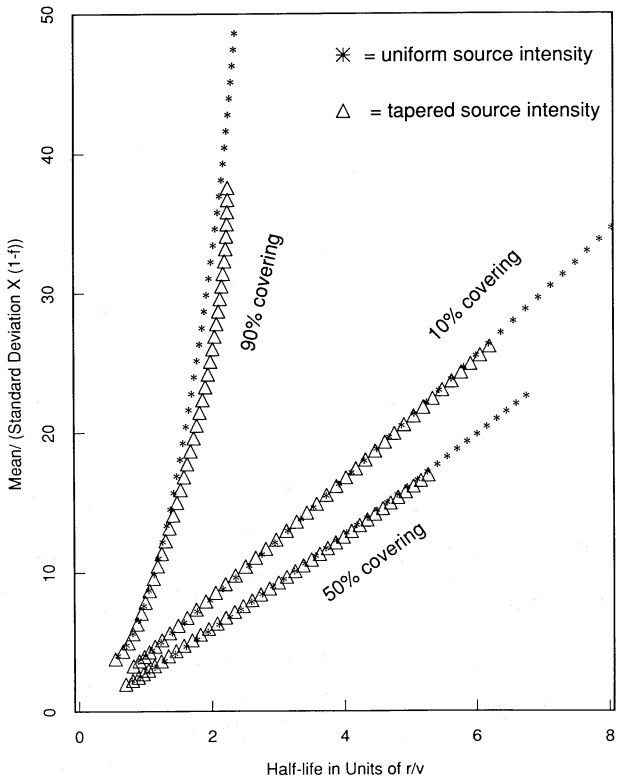

FIG. 5.—Comparison of predictions from uniform (*stars*) and from tapered (*triangles*) source intensity functions. For the tapered case, the X-ray surface brightness declines linearly along the radius from the center. The predictions shown for three values of mean covering fraction are contours like those in Fig. 4.

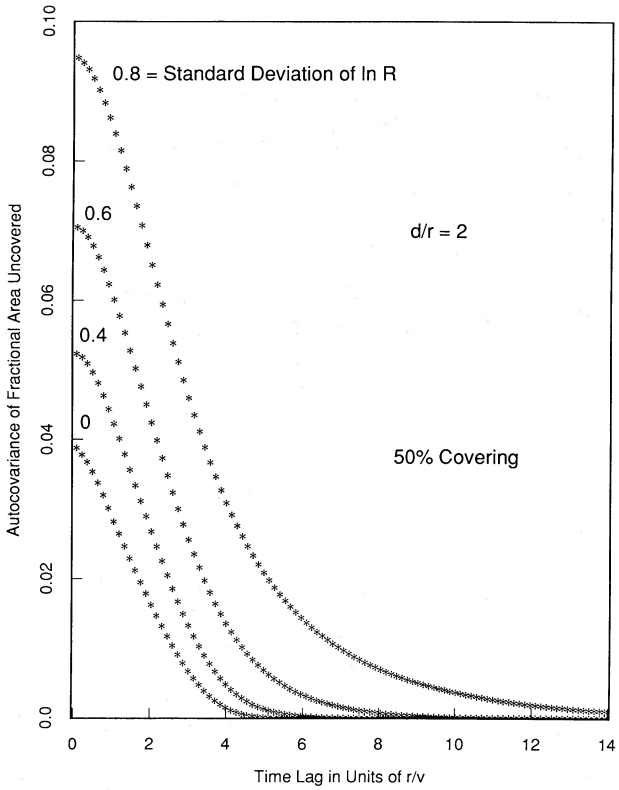

FIG. 6.—Dependence of a predicted autocovariance function on the variability assumed for cloud radii. The example of Fig. 2, with 50% mean covering, is plotted together with cases in which the standard deviation of the logarithm of cloud radius varies from 0.4 to 0.8, while the source radius is held constant at twice the root-mean-squared cloud radius.

discrete approximation to a normal distribution. The mean of this approximate normal distribution is equal to the negative of its standard deviation. This is necessary for the expected cloud area to be kept at the same value πr^2, so that the mean covering fraction f remain the same in all cases. In this plot, $f = 50\%$ and $d/r = 2$. The discrete approximation is concentrated on nine values of R, chosen with a generous representation of values in the upper tail of the distribution in order to make the discrete approximation of $\int R^2 h(R) dR$ a good one. The four curves in Figure 6 correspond to standard deviations σ_R of 0.8, 0.6, 0.4, and 0.0 in the underlying log-normal distribution. In the extreme case of a standard deviation of 0.8, the distribution of radii spreads over a factor of 20, from $0.4r$ to $9.4r$. The curve for $\sigma_R = 0$ is the same fixed-radius curve as in Figure 2.

The effect of random radius is to increase both the ratio of covariance to squared mean on the ordinate, and the half-life in units of r/v on the abscissa, shifting the autocovariance functions up and to the right. This is not surprising. The huge clouds that do occur, no matter how infrequently, produce occasional stretches of high obscuration with long persistence. Averaged with the more frequent small clouds, these huge clouds extend the amplitude and the time scale of variability, and give a long tail to the autocovariance, compared with the $\sigma_R = 0$ case.

For the case of 50% covering, the half-life is reasonably well fitted by

$$\tau_{1/2} = 2.3r/v + 2.0d/v \quad \text{when} \quad \sigma_R = 0.8 ,$$

compared with

$$\tau_{1/2} = 0.56r/v + 0.62d/v \quad \text{when} \quad \sigma_R = 0 .$$

For ratios of $d/r \lesssim 2$, the quantity Ω is given for 50% covering by

$$\Omega = 1.3 + 0.89d/r \quad \text{when} \quad \sigma_R = 0.8 ,$$

compared with

$$\Omega = 0.51 + 1.07d/r \quad \text{when} \quad \sigma_R = 0 .$$

The calculations of d and r from observables discussed in § IV can be repeated for any given value of σ_R, or any alternative distribution of source radius. For example, if the observed value of Ω is 2.5 and $f = 0.9$, as in the example discussed in § V, the estimate of d/r decreases from 5.3 for clouds of fixed radius to 3.5 for clouds of random radius, with the extreme value $\sigma_R = 0.8$. The half-life in terms of r/v shoots up from 1.7 to 9.0. If the observed half-life is 0.5 day, the estimate of source radius d drops nearly one order of magnitude, from 4×10^{13} cm to 6.8×10^{12} cm. The estimate of r, which is now the radius of a cloud of average area, drops from 0.7×10^{13} cm to 1.5×10^{12} cm as σ_R ranges from 0.0 to 0.8. Thus, a large dispersion in cloud sizes has a substantial effect on estimates of d and r.

If a soft X-ray light curve is sufficiently long to permit an estimate of the autocovariance function accurate to the point at which it drops to ~ 0.1 of its initial value, then its shape can provide clues to distinguish cases of low and high σ_R in cloud radii. The general effect of giving an appreciable dispersion to broad-line cloud sizes, for the ranges of parameters treated above, is to lengthen the tail of the autocovariance function. The ratio of "three-quarter life" to "one-quarter life" of the autocorrelation function is easily predicted from the geometric models, and might be a useful index from which to recognize, in individual cases, the effects of random cloud radii.

c) *Cloud Opacities*

The finite optical depth of clouds with low to moderate column densities also affects the predictions of our model. The effect on the mean covering fraction is readily calculated. Imagine that in the energy passband used for the observations, an individual cloud has an effective optical depth τ. The mean flux received, F, is given by

$$F \propto \sum_{q=0}^{\infty} \left[\frac{(\lambda \pi r^2)^q}{q!} e^{-\lambda \pi r^2} \right] e^{-q\tau} , \tag{20}$$

where the factor in brackets is the expected fractional area covered by q clouds under the Poisson hypothesis. The sum in equation (20) is just the expansion of an exponential, yielding

$$F \propto \exp \left[-\lambda \pi r^2 (1 - e^{-\tau}) \right] . \tag{21}$$

Thus, for example, if the covering fraction is 0.9, then $\lambda \pi r^2 \approx 2.3$; if $\tau = 1$, then the mean flux received is greater than in the case of infinite optical depth by a factor of 2.3.

Similarly, the results of § IV can be revised to incorporate the optical depth of clouds as a parameter. In effect, all we need to do is rescale the cloud intensity λ in equation (16). Thus, the λ in the factor in brackets is replaced by $\lambda(1 - e^{-\tau})^2$. The effect on the mean, as we have seen, is equivalent to replacing λ by the different quantity $\lambda(1 - e^{-\tau})$. By equation (1), this is equivalent to a rescaling of f:

$$f \rightarrow 1 - (1 - f)^{(1 - e^{-\tau})} . \tag{22}$$

Consequently, the effect of finite τ on the predictions of Figure 4 is to replace a curve calculated for an observed value of f by a revised value given by equation (22).

As an example, imagine that f for a given source is measured to be 90%, and a light curve is observed in a passband with effective optical depth 0.5. According to equation (22), we should use the $f = 60\%$ curve in Figure 4. The scale on the ordinate remains unchanged, and our previous example with $\Omega/(1 - f) = 25$ and an observed half-life of 0.5 day leads to the estimates $d/r = 10$ rather than 5 in the infinite optical depth case, $r = 0.2 \times 10^{13}$ cm rather than 0.7×10^{13} cm, and $d = 2 \times 10^{13}$ cm rather than 4×10^{13} cm.

If clouds have randomly distributed radii and are spherical rather than pancake shaped, then optical depth will be a function of the radius of the clouds. In principle, light curves in different passbands will carry information about clouds of different column densities, allowing us to probe the nature of the broad-line clouds in more detail. An additional complication is the fact that the optical depth of a spherical cloud is a function of the distance a light ray passes from its center. Such refinements go beyond the scope of the present paper.

VII. SUMMARY AND DISCUSSION

We have developed a model to explain the observed soft X-ray variability of some low-luminosity Seyfert 1 galaxies. The variability is due to changes in the covering fraction of the central source as broad-line clouds move across our line of sight. Our work is the natural extension of the analysis presented by Reichert, Mushotzky, and Holt (1986). Although much of the soft X-ray variability in AGNs may be unrelated to the process investigated in this paper, we emphasize that at least *some* of it must be, given the existence of dense clouds in the BLR and a reasonably well-defined source of soft X-rays. It is quite possible that objects exist in which variable covering fraction produces most of the observed variations in soft X-ray flux.

The formalism developed in this paper is used to demonstrate how analysis of a soft X-ray light curve can provide three important quantities: the radius of the X-ray–emitting region, the radius of a typical broad-line cloud, and the electron density in the cloud. The first of these may be combined with measurements of the total X-ray flux to derive the Eddington ratio, $L_X/L_{\rm Edd}$. Our estimates are quite insensitive to effects of nonuniform sources, but relaxing our assumption that all broad-line clouds have the same size affects the results substantially. The effects of having a distribution of cloud sizes, however, can in principle be seen in the autocorrelation function of the soft X-ray light curve.

The formulae in § IV are well suited not only to the assessment of such systematic errors, but also to Monte Carlo predictions of sampling errors. A thorough study of sampling errors is important for the design of observational strategies for the future. This, unfortunately, is a large subject; there are many competing factors and tradeoffs to consider. These include the amount of time a given source is observed versus the requirements of other projects, as well as the width of the adopted passband versus the effects produced by a wide range of cloud optical depths. There is nothing sacred about our choice of correlational half-life as the index of time scale of variability. It may be that a shorter baseline could be accommodated without much loss in estimation efficiency by taking correlational quarter-life or some other index. The feasibility of such a recourse depends on how random the radii of clouds are assumed to be; we saw in § VI that it is the long time-lag tail of the autocovariance function that carries information about the distribution in cloud sizes. In many cases, the uncertainties in the measurement of mean covering fractions for AGNs are likely to dominate other sources of error. A full study of such questions awaits a future paper.

Ideally we want long, uninterrupted, soft X-ray light curves with frequent temporal sampling in order to carry out the proposed analysis. Thus, an AGN should be observed frequently enough that even the shortest variability time scales are adequately sampled,

over a period of time long enough that low temporal frequencies are covered. For a typical Seyfert galaxy, one week of continuous observations may be a reasonable goal, but this may mean that observations of other objects must be sacrificed. An example of what can be done is provided by Lawrence *et al.* (1987) in the case of NGC 4051, but we saw in § II that this galaxy does not have suitable characteristics for our purposes.

It is important to choose an X-ray passband in which the broad-line clouds have high optical depths, since the variability is reduced if the clouds are somewhat transparent. The passband should also exclude any known soft X-ray excesses; it is likely that they arise from a physically distinct region of the AGN and are not subject to absorption from the moving broad-line clouds (Filippenko and Halpern 1988). Simultaneous hard X-ray light curves may sometimes allow us to distinguish between *intrinsic* variability, perhaps due to a changing rate of accretion onto the central source, and *extrinsic* variability, due to fluctuations in the covering fraction of broad-line clouds. On the other hand, if the soft and hard X-rays are produced by intrinsically different mechanisms, it will be difficult to prove that the soft X-ray variability in a given object *must* be caused by motions of broad-line clouds.

We eagerly look forward to the publication of more X-ray light curves and spectra from *EXOSAT*, and we urge observers to obtain high-quality data for at least a few of the most appropriate low-luminosity Seyfert 1 nuclei with *Ginga* and *Kvant*. Eventually, *ROSAT*, *XMM*, and *AXAF* will provide the largest and most complete set of observations for many AGNs. It will then be possible to derive the parameters discussed above for a substantial number of objects, and to study the systematic properties of the BLR.

A. V. F. received financial assistance from CalSpace grant CS-27-87. M. A. S. gratefully acknowledges the support of an NSF Graduate Fellowship and a Berkeley Graduate Fellowship. We thank Joe Silk for many useful discussions that led to the formulation of this problem, Peter Hall for insight into the approach to the Poisson limit, Andy Lawrence for pointing out several recent references on *EXOSAT* observations, and Claude Canizares, the referee, for some very important comments. Useful suggestions were also provided by David Band, Jules Halpern, Chris McKee, and Roger Romani.

APPENDIX

AREA OF POLYGONS FORMED BY A POISSON LINE PROCESS IN THE PLANE

Here we consider the area of polygons formed by a Poisson line process in the plane. This problem was first solved in the context of cloud-chamber tracks by Goudsmit (1945); the present discussion follows Kendall and Moran (1963). We imagine the Poisson line process in the plane to be the limiting case of the problem of great circles placed randomly on the surface of a unit sphere. Each circle can be defined by the coordinates of its two poles on the surface of the sphere; the equator, for example, is defined by the North and South poles. Thus, our random hypothesis simply means that the poles are distributed randomly over the surface of the sphere.

Let n be the number of great circles. The first one placed down creates two distinct regions on the sphere. In the nondegenerate case, the second circle cuts each of these regions in two, thereby producing four regions, and the third circle makes eight regions. Similarly, circle $n + 1$ intersects all n other circles, and thus creates $2n$ new regions. By induction, the total number of regions is $2 + n(n - 1)$ when n great circles are placed on the sphere. We also deduce that the number of segments into which the great circles are chopped is $2n(n - 1)$. Since each is a border to two regions, the average number of sides per region is

$$\frac{4n(n-1)}{2+n(n-1)},$$

which approaches 4 as n becomes large. The total surface area of the unit sphere is 4π; thus, the average area of a region approaches $4\pi n^{-2}$ for large n.

Now consider a small circle of radius ρ and center P on the surface of the sphere. A great circle that intersects this small circle is one whose perpendicular distance from P is less than ρ. The locus of the most distant of the two poles of such great circles traces out a thin ribbon of thickness ρ on the sphere. The nearest edge of this ribbon is a great circle itself, with pole P, and the area of the ribbon is close to $2\pi\rho$. The number of great circles that intersect the small circle is ρn, the ratio of the ribbon's area to that of the hemisphere multiplied by n. Proceeding to the limit of large n and small ρ, we can treat the small circle as a plane circle and equate ρn to $2\pi\rho\kappa$, where κ is the intensity of the Poisson line process for the plane region (as defined in the text). Hence $n = 2\pi\kappa$, and the average area of each region ($4\pi n^{-2}$) is simply $(\pi\kappa^2)^{-1}$, as we wished to show.

REFERENCES

Barr, P., *et al.* 1977, *M.N.R.A.S.*, **181**, 43P.
Barr, P., and Giommi, P. 1985, *IAU Circ.*, No. 4044.
Barr, P., Giommi, P., Wamsteker, W., Gilmozzi, R., and Mushotzky, R. F. 1985, *Bull. AAS*, **17**, 608.
Barr, P., and Mushotzky, R. F. 1986, *Nature*, **320**, 421.
Bassani, L., Dean, A. J., and Sembay, S. 1983, *Astr. Ap.*, **125**, 52.
Becker, R., and Chambers, J. M. 1984, *S: An Interactive Environment for Data Analysis and Graphics* (Belmont, CA: Wadsworth).
Blandford, R. D., and Königl, A. 1979, *Ap. J.*, **232**, 34.
Branduari-Raymont, G. 1986, in *The Physics of Accretion onto Compact Objects*, ed. K. O. Mason, M. G. Watson, and N. E. White (Berlin: Springer), p. 407.
Canizares, C. R., Kriss, G. A., Kruper, J., and Urry, C. M. 1986, in *IAU Symposium 119, Quasars*, ed. G. Swarup and V. K. Kapahi (Dordrecht: Reidel), p. 253.
Davidson, K., and Netzer, H. 1979, *Rev. Mod. Phys.*, **51**, 715.
Elvis, M., and Lawrence, A. 1985, in *Astrophysics of Active Galaxies and Quasi-Stellar Objects*, ed. J. S. Miller (Mill Valley, CA: University Science Books), p. 289.
Elvis, M., Maccacaro, T., Wilson, A., Ward, M., Penston, M., Fosbury, R., and Perola, G. C. 1978, *M.N.R.A.S.*, **183**, 129.
Feigelson, E. D., *et al.* 1986, *Ap. J.*, **302**, 337.
Filippenko, A. V. 1988, in *Supermassive Black Holes*, ed. M. Kafatos (Cambridge: Cambridge University Press), p. 104.

Filippenko, A. V., and Halpern, J. P. 1988, in preparation.
Filippenko, A. V., and Sargent, W. L. W. 1988, *Ap. J.*, **324**, 134.
Goldstein, H. 1980, *Classical Mechanics* (2d ed., Reading, MA: Addison-Wesley), pp. 426–428.
Goudsmit, S. 1945, *Rev. Mod. Phys.*, **17**, 321.
Hall, P. 1985, *Zs. Wahrscheinlichkeitstheorie ver. Gebiete*, **70**, 237.
Halpern, J. P. 1982, Ph.D. thesis, Harvard University.
———. 1984, *Ap. J.*, **281**, 90.
Halpern, J. P., and Steiner, J. E. 1983, *Ap. J. (Letters)*, **269**, L37.
Holt, S. S., Mushotzky, R. F., Becker, R. H., Boldt, E. A., Serlemitsos, P. J., Szymkowiak, A. E., and White, N. E. 1980, *Ap. J. (Letters)*, **241**, L13.
Kendall, M. G., and Moran, P. A. P. 1963, *Geometrical Probability* (London: Griffith).
Krolik, J. H., McKee, C. F., and Tarter, C. B. 1981, *Ap. J.*, **249**, 422.
Kwan, J., and Krolik, J. H. 1981, *Ap. J.*, **250**, 478.
Lawrence, A., and Elvis, M. 1982, *Ap. J.*, **256**, 410.
Lawrence, A., Watson, M. G., Pounds, K. A., and Elvis, M. 1985, *M.N.R.A.S.*, **217**, 685.
———. 1987, *Nature*, **325**, 694.
Lightman, A. P., Giacconi, R., and Tananbaum, H. 1978, *Ap. J.*, **224**, 375.
Longair, M. S. 1981, *High Energy Astrophysics* (Cambridge: Cambridge University Press).
Malkan, M. A. 1983, *Ap. J.*, **268**, 582.
Moran, P. A. P., and Fazekas de St. Groth, S. 1962, *Biometrika*, **49**, 389.
Mushotzky, R. F. 1982, *Ap. J.*, **256**, 92.
Mushotzky, R. F., Holt, S. S., and Serlemitsos, P. J. 1978, *Ap. J. (Letters)*, **225**, L115.
Osterbrock, D. E., and Mathews, W. G. 1986, *Ann. Rev. Astr. Ap.*, **24**, 171.
Perola, G. C., *et al.* 1986, *Ap. J.*, **306**, 508.
Phinney, E. S. 1985, in *Astrophysics of Active Galaxies and Quasi-Stellar Objects*, ed. J. S. Miller (Mill Valley, CA: University Science Books), p. 453.
Pounds, K. A. 1979, *Proc. Roy. Soc. London A*, **366**, 375.
Pounds, K. A., and Turner, T. J. 1987, in *Variability of Galactic and Extragalactic X-Ray Sources*, ed. A. Treves (Milano: Associazione per L'Avanzamento Dell'Astronomia), p. 1.
Pounds, K. A., Warwick, R. S., Culhane, J. L., and de Korte, P. A. J. 1986, *M.N.R.A.S.*, **218**, 685.
Puetter, R. C. 1986, in *IAU Symposium 119, Quasars*, ed. G. Swarup and V. K. Kapahi (Dordrecht: Reidel), p. 341.
Reichert, G. A., Mushotzky, R. F., and Holt, S. S. 1986, *Ap. J.*, **303**, 87 (RMH).
Reichert, G. A., Mushotzky, R. F., Petre, R., and Holt, S. S. 1985, *Ap. J.*, **296**, 69.
Schwartz, D. 1987, *Ap. J.*, **318**, 568.
Shakura, N. I., and Sunyaev, R. A. 1973, *Astr. Ap.*, **24**, 337.
Tananbaum, H., Peters, G., Forman, W., Giacconi, R., Jones, C., and Avni, Y. 1978, *Ap. J.*, **223**, 74.
Tennant, A. F., and Mushotzky, R. F. 1983, *Ap. J.*, **264**, 92.
Tennant, A. F., Mushotzky, R. F., Boldt, E. A., and Swank, J. H. 1981, *Ap. J.*, **251**, 15.
Wandel, A., and Mushotzky, R. F. 1986, *Ap. J. (Letters)*, **306**, L61.
Wandel, A., and Yahil, A. 1986, *Ap. J. (Letters)*, **295**, L1.
Warwick, R. S. 1986, in *The Physics of Accretion onto Compact Objects*, ed. K. O. Mason, M. G. Watson, and N. E. White (Berlin: Springer), p. 195.
Whitehouse, D. R., and Cruise, A. M. 1985, *Nature*, **315**, 554.
Wilkes, B. J., and Elvis, M. 1987, *Ap. J.*, **323**, 243.
Worrall, D. M., *et al.* 1982, *Ap. J.*, **261**, 403.

ALEXEI V. FILIPPENKO and MICHAEL A. STRAUSS: Department of Astronomy, University of California, Berkeley, CA 94720

KENNETH W. WACHTER: Department of Statistics, University of California, Berkeley, CA 94720